

Zinc-Containing Carboxylate-Bridged Heterodimetallic Complexes and Their Reactions with Phosphodiester Ligands

Tomoaki Tanase,[†] Joanne W. Yun, and Stephen J. Lippard*

Department of Chemistry, Massachusetts Institute of Technology, Cambridge, Massachusetts 02139

Received December 19, 1995[⊗]

A series of zinc-containing heterodimetallic complexes were prepared by using the dinucleating ligand XDK [$\text{H}_2\text{XDK} = m\text{-xylylenediamine bis(Kemp's triacid imide)}$]. Mononuclear $[\text{Zn}(\text{XDK})(\text{H}_2\text{O})]$ (**1**) reacts with 1 equiv of $\text{M}(\text{acac})_2 \cdot 2\text{H}_2\text{O}$ ($\text{acac} = 2,4\text{-pentanedionate}$) to afford the heterodimetallic compounds $[\text{Zn}^{\text{II}}\text{M}^{\text{II}}(\text{XDK})(\text{acac})_2(\text{CH}_3\text{OH})_2] \cdot \text{H}_2\text{O}$ (**2**· H_2O , $\text{M} = \text{Co}$, 65% isolated yield; **3**· H_2O , $\text{M} = \text{Mn}$, 54%; **4**· H_2O , $\text{M} = \text{Fe}$, 30%; **5**· H_2O , $\text{M} = \text{Ni}$, 32%). As determined by X-ray crystallography, **2–5** each contain a $\text{Zn}^{\text{II}}\text{M}^{\text{II}}$ dinuclear core bridged by XDK and acac ligands. The zinc and M atoms have trigonal bipyramidal and octahedral geometries, respectively. The $\text{Zn} \cdots \text{M}$ separations depend on the metal ion in the octahedral site (**2**, $\text{M} = \text{Co}$, 3.440(2) Å; **3**, $\text{M} = \text{Mn}$, 3.517(1) Å; **4**, $\text{M} = \text{Fe}$, 3.492(1) Å; **5**, $\text{M} = \text{Ni}$, 3.397(1) Å), a variation which is correlated with the ionic radius of the high-spin octahedral metal ion. The reaction of **2** with diphenyl hydrogen phosphate afforded the bis(phosphate) complex $[\text{ZnCo}(\text{XDK})\{\mu\text{-}\eta^2\text{-(PhO)}_2\text{PO}_2\}\{\eta^1\text{-(PhO)}_2\text{PO}_2\}(\text{CH}_3\text{OH})_2(\text{H}_2\text{O})]$ (**7**, 49% yield). The ZnCo center is bridged by the XDK through its two carboxylate groups and by a diphenyl phosphate ligand. The other diphenyl phosphate is terminally coordinated to the zinc atom in a monodentate fashion. The $\text{Zn} \cdots \text{Co}$ interatomic distance is 3.846(1) Å. An analogous bis(phosphate) homodinuclear complex, $[\text{Zn}_2(\text{XDK})\{\mu\text{-}\eta^2\text{-(PhO)}_2\text{PO}_2\}\{\eta^1\text{-(PhO)}_2\text{PO}_2\}(\text{CH}_3\text{OH})_2(\text{H}_2\text{O})]$ (**8**), was prepared by reacting $[\text{Zn}_2(\text{XDK})(\text{acac})_2(\text{CH}_3\text{OH})_2]$ (**6**) with diphenyl hydrogen phosphate in 64% yield. Compound **8**, which is isomorphous with **7**, has an asymmetrical dizinc core bridged by XDK and a phosphate ligand ($\text{Zn} \cdots \text{Zn} = 3.869(2)$ Å). The monodentate diphenyl phosphate ligand dissociates from the dimetallic center of **8** in solution, as revealed by molar conductivity and ^1H and $^{31}\text{P}\{^1\text{H}\}$ NMR spectroscopic studies. The resulting free phosphate ligand exchanges with the bridging one in methanol- d_4 . The present results provide a useful synthetic route to carboxylate-bridged heterodimetallic compounds, which are potential models for the active centers in nonredox metalloproteins. Crystal data are as follows. **2**: monoclinic, $P2_1/c$, $a = 17.725(7)$ Å, $b = 12.354(4)$ Å, $c = 21.815(6)$ Å, $\beta = 90.45(3)^\circ$, $V = 4777(2)$ Å³, $Z = 4$; $R = 0.049$ and $R_w = 0.051$ for 3884 reflections with $I > 3\sigma(I)$. **3**: monoclinic, $P2_1/c$, $a = 17.292(2)$ Å, $b = 12.450(1)$ Å, $c = 21.717(2)$ Å, $\beta = 91.464(7)^\circ$, $V = 4673.9(7)$ Å³, $Z = 4$; $R = 0.046$ and $R_w = 0.051$ for 3876 reflections. **4**: monoclinic, $P2_1/c$, $a = 17.630(1)$ Å, $b = 12.374(2)$ Å, $c = 21.771(2)$ Å, $\beta = 90.306(8)^\circ$, $V = 4749.4(7)$ Å³, $Z = 4$; $R = 0.041$ and $R_w = 0.049$ for 3248 reflections. **5**: monoclinic, $P2_1/c$, $a = 17.817(2)$ Å, $b = 12.241(3)$ Å, $c = 21.786(2)$ Å, $\beta = 91.043(9)^\circ$, $V = 4751(1)$ Å³, $Z = 4$; $R = 0.050$ and $R_w = 0.058$ for 4497 reflections. **7**· CH_3OH : monoclinic, $P2_1/n$, $a = 18.812(2)$ Å, $b = 16.156(2)$ Å, $c = 21.760(2)$ Å, $\beta = 112.836(9)^\circ$, $V = 6095(1)$ Å³, $Z = 4$; $R = 0.055$ and $R_w = 0.064$ for 5843 reflections. **8**· CH_3OH : monoclinic, $P2_1/n$, $a = 18.845(6)$ Å, $b = 16.105(3)$ Å, $c = 21.776(3)$ Å, $\beta = 112.78(2)^\circ$, $V = 6091(2)$ Å³, $Z = 4$; $R = 0.055$ and $R_w = 0.061$ for 5189 reflections.

Introduction

Metalloenzymes with zinc-containing dimetallic centers are the subject of much current attention. Recent structural studies of proteins in this class having carboxylate-bridged heterodimetallic cores have generated interest in understanding how the geometry of this motif relates to its function. Included among these enzymes are the Klenow fragment of DNA polymerase I from *Escherichia coli* (with a $\text{Zn}(\text{II})/\text{Mg}(\text{II})$ center),¹ *E. coli* alkaline phosphatase ($2\text{Zn}(\text{II})/\text{Mg}(\text{II})$ or $3\text{Zn}(\text{II})$),² *Thermus aquaticus* DNA polymerase (*Taq* polymerase) ($\text{Zn}(\text{II})/2\text{Mn}(\text{II})$),³ bovine lens leucine aminopeptidase (bLAP) ($\text{Zn}(\text{II})/\text{Mg}(\text{II})$ or

$2\text{Zn}(\text{II})$),⁴ kidney bean purple acid phosphatase (KBAP) ($\text{Zn}(\text{II})/\text{Fe}(\text{III})$),⁵ and calcineurin ($\text{Zn}(\text{II})/\text{Fe}(\text{III})$).⁶ Enzymes employing heterodimetallic active sites seem to take advantage of the different labilities and/or Lewis acidities of the disparate metal ions. For example, the Klenow fragment of DNA polymerase I, which can also function with either two $\text{Zn}(\text{II})$ or two $\text{Mg}(\text{II})$ ions, employs a $\text{Zn}(\text{II})/\text{Mg}(\text{II})$ active site. The zinc ion is postulated to generate a nucleophile from coordinated water while the magnesium ion stabilizes the pentacoordinate transition state at phosphorus, neutralizing the negative charge built up on the leaving group.¹ The $\text{Zn}(\text{II})/\text{Fe}(\text{III})$ dinuclear core of KBAP similarly hydrolyzes activated phosphoric acid esters

[†] Permanent address: Department of Chemistry, Faculty of Science, Toho University, Miyama 2-2-1, Funabashi, Chiba 274, Japan.

[⊗] Abstract published in *Advance ACS Abstracts*, May 1, 1996.

- (1) (a) Freemont, P. S.; Friedman, J. M.; Beese, L. S.; Sanderson, M. R.; Steitz, T. A. *Proc. Natl. Acad. Sci. U.S.A.* **1988**, *85*, 8924. (b) Beese, L. S.; Steitz, T. A. *EMBO J.* **1991**, *10*, 25.
- (2) (a) Sowadski, J. M.; Handschumacher, M. D.; Murthy, H. M. K.; Foster, B. A.; Wyckoff, H. W. *J. Mol. Biol.* **1985**, *186*, 417. (b) Kim, E. E.; Wyckoff, H. W. *J. Mol. Biol.* **1991**, *218*, 449.
- (3) Kim, Y.; Eom, S. H.; Wang, J.; Lee, D.-S.; Suh, S. W.; Steitz, T. A. *Nature* **1995**, *376*, 612.

- (4) (a) Burley, S. K.; David, P. R.; Taylor, A.; Lipscomb, W. M. *Proc. Natl. Acad. Sci. U.S.A.* **1990**, *87*, 6878. (b) Burley, S. K.; David, P. R.; Lipscomb, W. N. *Proc. Natl. Acad. Sci. U.S.A.* **1991**, *88*, 6916. (c) Burley, S. K.; David, P. R.; Sweet, R. M.; Taylor, A.; Lipscomb, W. N. *J. Mol. Biol.* **1992**, *224*, 113. (d) Kim, H.; Lipscomb, W. N. *Proc. Natl. Acad. Sci. U.S.A.* **1993**, *90*, 5006.
- (5) Sträter, N.; Klabunde, T.; Tucker, P.; Witzel, H.; Krebs, B. *Science* **1995**, *268*, 1489.
- (6) Griffith, J. P.; Kim, J. L.; Kim, E. E.; Sintchak, M. D.; Thomson, J. A.; Fitzgibbon, M. J.; Fleming, M. A.; Caron, P. R.; Hsiao, K.; Navia, M. A. *Cell* **1995**, *82*, 507.

in a mechanism involving hydroxide ion bound to Fe(III).⁵ Calcineurin, which plays an important role in signal transduction pathways in the cell, is a target of immunosuppressant drugs used, for example, to prevent rejection following organ transplants.⁶ Understanding the mechanism of phosphatase activity at the carboxylate-bridged heterometallic core of this Zn(II)/Fe(III)-containing enzyme therefore has practical implications.

Apart from their biological relevance, new routes to carboxylate-bridged heterodimetallic complexes, especially those comprising two divalent metal ions, are desirable. Few such compounds have been structurally characterized and efficient syntheses are rare. Symmetric and asymmetric $[MM'(\mu-O)(\mu\text{-acetate})_2L_2]^{n+}$ and $[MM'(\mu-OH)(\mu\text{-acetate})_2L_2]^{n+}$ complexes, where M, M' = a first-row transition metal or Ru and L = 1,4,7-trimethyl-1,4,7-triazacyclononane (Me₃tacn) and/or 1,4,7-triazacyclononane (tacn), can be obtained from the mononuclear $\{ML\}^{n+}$ precursors.⁷ The magnetic and spectroscopic properties of these complexes have been investigated mainly in the oxidation states, M^{III}M^{II}, M^{III}M^{III}, and M^{III}M^{IV}, where M = Cr, Fe, or Ru. A series of Cu(II)-containing heterodinuclear complexes, $[Cu^{II}(\text{Dopn})(\mu\text{-CH}_3\text{CO}_2)ML]^{n+}$, where H₂Dopn = 3,9-dimethyl-4,8-diazaundeca-3,8-diene-2,10-dione dioxime and M = Mn(II), Co(II), Ni(II), Mn(III), or Fe(III), are also known.⁸ Heterodimetallic complexes of the kind $[FeM(\text{BPMP})(\mu\text{-carboxylate})_2]^{n+}$ (HBPMP = 2,6-bis[bis(2-pyridylmethyl)-amino]methyl]-4-methylphenol) are available for Fe^{III}M^{II} (M = Ni, Zn, Mn, Cu), Fe^{II}M^{II} (M = Mn, Co, Zn), and Fe^{II}Ga^{III}.⁹

Recently, we reported the preparation of the mononuclear Co(II) and Zn(II) complexes $[Co(\text{XDK})(\text{neocuproine})]^{10}$ and $[Zn(\text{XDK})(\text{H}_2\text{O})]^{11}$ (**1**), where H₂XDK is *m*-xylylenediamine bis(Kemp's triacid imide) and neocuproine is 2,9-dimethyl-1,10-phenanthroline. The former was converted to the heterodimetallic compound $[KCo(\text{XDK})(\text{neocuproine})(\text{PF}_6)]$ by treatment with KPF₆,¹⁰ and the latter proved to be a good precursor of the dizinc complexes $[Zn_2(\text{XDK})(\text{NO}_3)_2(\text{py})_2]$ and $[Zn_2(\text{XDK})(\text{acac})_2(\text{CH}_3\text{OH})_2]$ (**6**) (acac = 2,4-pentanedionate).¹¹ The dinucleating ligand XDK also stabilizes Fe^{II}₂, Fe^{III}₂, Co^{II}₂, Mg^{II}₂, Mn^{II}₂, and Mn^{III}₂ complexes.^{12,13} Here, we describe a

general route to carboxylate-bridged zinc-containing heterodimetallic complexes, $[ZnM(\text{XDK})(\text{acac})_2(\text{CH}_3\text{OH})_2]$ (M = Co²⁺, Mn²⁺, Fe²⁺, Ni²⁺), from the monozinc precursor **1**, and their transformation to novel bis(phosphate)-substituted complexes. A preliminary account appeared previously.^{11a}

Experimental Section

All manipulations except for the preparation of $[ZnFe(\text{XDK})(\text{acac})_2(\text{CH}_3\text{OH})_2]\cdot\text{H}_2\text{O}$ (**4**·H₂O) were carried out in air, and all reagents and solvents were used as received. *m*-Xylylenediamine bis(Kemp's triacid imide) (H₂XDK)¹⁴ and Fe(acac)₂·2H₂O (acac = 2,4-pentanedionate)¹⁵ were synthesized by known methods. The preparations of $[Zn(\text{XDK})(\text{H}_2\text{O})]$ (**1**) and $[Zn_2(\text{XDK})(\text{acac})_2(\text{CH}_3\text{OH})_2]\cdot\text{H}_2\text{O}$ (**6**·H₂O) were reported previously.¹¹

Measurements. NMR spectroscopic measurements were made on a Bruker AC250 or a Varian UNITY300 instrument. ¹H NMR spectra were measured at 250 or 300 MHz using tetramethylsilane as an external reference (chemical shifts were calibrated relative to solvent peaks), and ³¹P{¹H} NMR spectra were measured at 121 MHz using 85% H₃PO₄ as an external reference. A variable-temperature ³¹P{¹H} NMR spectroscopic study was performed on the Varian UNITY300 instrument; temperatures were calibrated by measuring ¹H NMR chemical shifts of methanol. Infrared and electronic absorption spectra were recorded on a Bio-Rad SPC 3200 and a Perkin-Elmer Lambda 7 spectrometer, respectively. Molar conductivity was measured at 24 °C in methanol by using a Fisher Scientific Model 9-326 conductivity bridge with a platinum-black electrode. Conductivities were recorded over a concentration range of 0.4–2.5 mM, which showed a linear correlation, and the reported molar conductivities (Ω⁻¹ cm² mol⁻¹) were derived from the slopes of a plot of conductivity (Ω⁻¹ cm⁻¹) versus concentration (mol cm⁻³). The electrolyte type was determined by reference to the molar conductivity of $[n\text{-Bu}_4\text{N}][\text{PF}_6]$ in methanol.

Preparation of $[ZnCo(\text{XDK})(\text{acac})_2(\text{CH}_3\text{OH})_2]\cdot\text{H}_2\text{O}$ (2**·H₂O).** The mononuclear complex $[Zn(\text{XDK})(\text{H}_2\text{O})]$ (**1**) (130 mg, 0.196 mmol) and Co(acac)₂·2H₂O (57 mg, 0.196 mmol) were refluxed in 25 mL of methanol for 30 min. The resultant violet solution was cooled to room temperature and was concentrated to ca. 2 mL to afford fine pink crystals of $[ZnCo(\text{XDK})(\text{acac})_2(\text{CH}_3\text{OH})_2]\cdot\text{H}_2\text{O}$ (**2**·H₂O), which were collected, washed with small amounts of ethanol and hexane, and dried in vacuo (125 mg, 65%). Anal. Calcd for C₄₄H₆₂N₂O₁₅ZnCo: C, 53.75; H, 6.36; N, 2.85; Zn, 6.65; Co, 5.99. Found: C, 53.60; H, 6.41; N, 2.80; Zn, 6.64; Co, 5.80. IR (Nujol): 3439 (br), 1728, 1680 (s), 1586 (s), 1520, 1191 (s), 1182 (s), 1026 (s), 959, 763 cm⁻¹. UV-vis (CHCl₃): λ_{max} (ε) 568 (3.9 × 10) nm (M⁻¹ cm⁻¹). ¹H NMR in CDCl₃ showed isotropically shifted features in the range -10 to +45 ppm.

Preparation of $[ZnMn(\text{XDK})(\text{acac})_2(\text{CH}_3\text{OH})_2]\cdot\text{H}_2\text{O}$ (3**·H₂O).** A methanolic solution (25 mL) containing $[Zn(\text{XDK})(\text{H}_2\text{O})]$ (**1**) (200 mg, 0.302 mmol) and Mn(acac)₂·2H₂O (87 mg, 0.301 mmol) was refluxed for 30 min. The resultant pale yellow solution was cooled to room temperature, passed through a glass filter, and concentrated to ca. 5 mL to give fine pale yellow crystals of $[ZnMn(\text{XDK})(\text{acac})_2(\text{CH}_3\text{OH})_2]\cdot\text{H}_2\text{O}$ (**2**·H₂O), which were collected, washed with small amounts of ethanol and hexane, and dried in vacuo (159 mg, 54%). Anal. Calcd for C₄₄H₆₂N₂O₁₅ZnMn: C, 53.97; H, 6.38; N, 2.86; Zn, 6.68; Mn, 5.61. Found: C, 53.63; H, 6.01; N, 2.89; Zn, 6.90; Mn, 5.97. IR (Nujol): 3428 (br), 1731, 1678 (s), 1591 (s), 1516, 1191 (s), 1182 (s), 1016 (s), 957, 764 cm⁻¹.

Preparation of $[ZnFe(\text{XDK})(\text{acac})_2(\text{CH}_3\text{OH})_2]\cdot\text{H}_2\text{O}$ (4**·H₂O).** All manipulations were carried out under a nitrogen atmosphere by using standard Schlenk techniques, and methanol was degassed prior to use. $[Zn(\text{XDK})(\text{H}_2\text{O})]$ (**1**) (275 mg, 0.415 mmol) and Fe(acac)₂·2H₂O (120 mg, 0.414 mmol) were refluxed in 25 mL of methanol for 30 min. The resultant dark yellow solution was cooled to room temperature and

- (7) (a) Chaudhuri, P.; Winter, M.; Küppers, H.-J.; Wieghardt, K.; Nuber, B.; Weiss, J. *Inorg. Chem.* **1987**, *26*, 3302. (b) Bossek, U.; Weyhermüller, T.; Wieghardt, K.; Bonvoisin, J.; Girerd, J. J. *J. Chem. Soc., Chem. Commun.* **1989**, 633. (c) Hotzelmann, R.; Wieghardt, K.; Flörke, U.; Haupt, H.-J. *Angew. Chem., Int. Ed. Engl.* **1990**, *29*, 645. (d) Hotzelmann, R.; Wieghardt, K.; Ensling, J.; Romstedt, H.; Gütllich, P.; Bill, E.; Flörke, U.; Haupt, H.-J. *J. Am. Chem. Soc.* **1992**, *114*, 9470. (e) Hotzelmann, R.; Wieghardt, K.; Flörke, U.; Haupt, H.-J.; Weatherburn, D. C.; Bonvoisin, J.; Blondin, G.; Girerd, J. J. *J. Am. Chem. Soc.* **1992**, *114*, 1681.
- (8) Birkelbach, F.; Winter, M.; Flörke, U.; Haupt, H.-J.; Butzlaff, C.; Lengen, M.; Bill, E.; Trautwein, A. X.; Wieghardt, K.; Chaudhuri, P. *Inorg. Chem.* **1994**, *33*, 3990.
- (9) (a) Borovik, A. S.; Que, L., Jr.; Papaefthymiou, V.; Münck, E.; Taylor, L. F.; Anderson, O. P. *J. Am. Chem. Soc.* **1988**, *110*, 1986. (b) Borovik, A. S.; Papaefthymiou, V.; Taylor, L. F.; Anderson, O. P.; Que, L., Jr. *J. Am. Chem. Soc.* **1989**, *111*, 6183. (c) Borovik, A. S.; Hendrich, M. P.; Holman, T. R.; Münck, E.; Papaefthymiou, V.; Que, L., Jr. *J. Am. Chem. Soc.* **1990**, *112*, 6031. (d) Holman, T. R.; Juarez-Garcia, C.; Hendrich, M. P.; Que, L., Jr.; Münck, E. *J. Am. Chem. Soc.* **1990**, *112*, 7611. (e) Wang, Z.; Holman, T. R.; Que, L., Jr. *Magn. Reson. Chem.* **1993**, *31*, S78. (f) Holman, T. R.; Wang, Z.; Hendrich, M. P.; Que, L., Jr. *Inorg. Chem.* **1995**, *34*, 134.
- (10) Watton, S. P.; Davis, M. I.; Pence, L. E.; Rebek, J., Jr.; Lippard, S. J. *Inorg. Chim. Acta* **1995**, *235*, 195.
- (11) (a) Tanase, T.; Watton, S. P.; Lippard, S. J. *J. Am. Chem. Soc.* **1994**, *116*, 9401. (b) Tanase, T.; Yun, J. W.; Lippard, S. J. *Inorg. Chem.* **1995**, *34*, 4220.
- (12) (a) Goldberg, D. P.; Watton, S. P.; Masschelein, A.; Wimmer, L.; Lippard, S. J. *J. Am. Chem. Soc.* **1993**, *115*, 5346. (b) Watton, S. P.; Masschelein, A.; Rebek, J., Jr.; Lippard, S. J. *J. Am. Chem. Soc.* **1994**, *116*, 5196. (c) Yun, J. W.; Tanase, T.; Pence, L. E.; Lippard, S. J. *J. Am. Chem. Soc.* **1995**, *117*, 4407. (d) Tanase, T.; Lippard, S. J. *Inorg. Chem.* **1995**, *34*, 4682.

- (13) (a) Hagen, K. S.; Lachicotte, R.; Kitaygorodskiy, A.; Elbouadili, A. *Angew. Chem., Int. Ed. Engl.* **1993**, *32*, 1321. (b) Hagen, K. S.; Lachicotte, R.; Kitaygorodskiy, A. *J. Am. Chem. Soc.* **1993**, *115*, 12617.
- (14) Rebek, J., Jr.; Marshall, L.; Wolak, R.; Parris, K.; Killoran, M.; Askew, B.; Nemeth, D.; Islam, N. *J. Am. Chem. Soc.* **1985**, *107*, 7476.
- (15) Buckingham, D. A.; Gorges, R. C.; Henry, J. T. *Aust. J. Chem.* **1967**, *20*, 281.

Table 1. Crystallographic and Experimental Data for [ZnM(XDK)(acac)₂(CH₃OH)₂] (**2**, M = Co; **3**, M = Mn; **4**, M = Fe; **5**, M = Ni)

	2	3	4	5
formula	C ₄₄ H ₆₀ N ₂ O ₁₄ ZnCo	C ₄₄ H ₆₀ N ₂ O ₁₄ ZnMn	C ₄₄ H ₆₀ N ₂ O ₁₄ ZnFe	C ₄₄ H ₆₀ N ₂ O ₁₄ ZnNi
fw	965.29	961.28	962.19	965.04
crystal system	monoclinic	monoclinic	monoclinic	monoclinic
space group	<i>P</i> 2 ₁ / <i>c</i>	<i>P</i> 2 ₁ / <i>c</i>	<i>P</i> 2 ₁ / <i>c</i>	<i>P</i> 2 ₁ / <i>c</i>
<i>a</i> , Å	17.725(7)	17.292(2)	17.630(1)	17.817(2)
<i>b</i> , Å	12.354(4)	12.450(1)	12.374(2)	12.241(3)
<i>c</i> , Å	21.815(6)	21.717(2)	21.771(2)	21.786(2)
β, deg	90.45(3)	91.464(7)	90.306(8)	91.043(9)
<i>V</i> , Å ³	4777(2)	4673.9(7)	4749.4(7)	4751(1)
<i>Z</i>	4	4	4	4
<i>T</i> , °C	-85	-110	-75	-79
<i>D</i> _{calcd} , g cm ⁻³	1.343	1.366	1.346	1.343
abs coeff, cm ⁻¹	9.16	8.49	8.75	9.66
transm factor	0.93–1.00	0.94–1.00	0.97–1.00	0.89–1.00
2θ range, deg	3 < 2θ < 45	3 < 2θ < 46	3 < 2θ < 40	3 < 2θ < 46
no. of unique data	6688	6976	4683	6958
no. of obsd data (<i>I</i> > 3σ(<i>I</i>))	3884	3876	3248	4497
no. of variables	560	560	560	560
<i>R</i> ^a	0.049	0.046	0.041	0.050
<i>R</i> _w ^a	0.051	0.051	0.049	0.058

^a $R = \sum ||F_o| - |F_c|| / \sum |F_o|$; $R_w = [\sum w(|F_o| - |F_c|)^2 / \sum w|F_o|^2]^{1/2}$, where $w = 1/\sigma^2(F_o)$. More details about the weighting scheme and other experimental protocols may be found in: Carnahan, E. M.; Rardin, R. L.; Bott, S. G.; Lippard, S. J. *Inorg. Chem.* **1992**, *31*, 5193.

concentrated to ca. 5 mL to give fine yellow crystals of [ZnFe(XDK)(acac)₂(CH₃OH)₂]·H₂O (**4**·H₂O), which were collected, washed with small amounts of hexane, and dried in vacuo (122 mg, 30%). Anal. Calcd for C₄₄H₆₀N₂O₁₅ZnFe: C, 53.92; H, 6.38; N, 2.86. Found: C, 53.33; H, 6.16; N, 2.92. IR (Nujol): 3461 (br), 1729, 1682 (s), 1586 (s), 1520, 1191 (s), 1182 (s), 1025 (s), 960, 764 cm⁻¹. UV-vis (CH₃OH): λ_{max} (ε) 442 (1.2 × 10³), 350 (1.8 × 10³) nm (M⁻¹ cm⁻¹).

Preparation of [ZnNi(XDK)(acac)₂(CH₃OH)₂]·H₂O (5**·H₂O).** Complex **1** (200 mg, 0.302 mmol) and Ni(acac)₂·2H₂O (88 mg, 0.300 mmol) were dissolved in 25 mL of methanol, and the solution was heated at reflux for 30 min. The resultant pale green solution was cooled to room temperature, passed through a glass filter, and concentrated to ca. 5 mL to afford a mixture of pale green crystals of the heterodimetallic compound and small amounts of Ni and Zn complexes of acac. The heterodimetallic complex was extracted with 20 mL of acetone. The acetone extract was passed through a glass filter and evaporated to dryness. The residue was crystallized from methanol to give fine pale green crystals of [ZnNi(XDK)(acac)₂(CH₃OH)₂]·H₂O (**5**·H₂O), which were collected, washed with small amounts of ethanol and hexane, and dried in vacuo (94 mg, 32%). Anal. Calcd for C₄₄H₆₀N₂O₁₅ZnNi: C, 53.76; H, 6.36; N, 2.85. Found: C, 53.85; H, 6.31; N, 3.00. IR (Nujol): 3460 (br), 1728, 1682 (s), 1587 (s), 1520, 1192 (s), 1182 (s), 1021 (s), 960, 764 cm⁻¹. UV-vis (CHCl₃): λ_{max} (ε) 688 (7.1 nm (M⁻¹ cm⁻¹)).

Preparation of [ZnCo(XDK){(PhO)₂PO₂}]₂(CH₃OH)₂(H₂O)] (7**).** To a solution of [ZnCo(XDK)(acac)₂(CH₃OH)₂]·H₂O (**2**·H₂O) (80 mg, 0.081 mmol) in methanol (10 mL)/methylene chloride (10 mL) was added diphenyl hydrogen phosphate (41 mg, 0.164 mmol). The reaction mixture was stirred at room temperature for 1 h. The solvent was then removed by a rotary evaporator, and the residue was crystallized from a CH₃OH/Et₂O mixed solvent. Large block-shaped pink crystals formed after several days and were collected, washed with ether, and dried in vacuo (51 mg, 49%). Anal. Calcd for C₅₈H₆₈N₂O₁₉ZnCoP₂ (**7**): C, 54.28; H, 5.34; N, 2.18. Found: C, 54.13; H, 5.00; N, 2.37. IR (Nujol): 3479 (br), 1731, 1681 (s), 1598 (s), 1592 (s), 1228, 1201 (s), 1118 (s), 930 (s), 764 (s), 722, 690 cm⁻¹. UV-vis (CHCl₃): λ_{max} (ε) 538 (1.7 × 10) nm (M⁻¹ cm⁻¹).

Preparation of [Zn₂(XDK){(PhO)₂PO₂}]₂(CH₃OH)₂(H₂O)] (8**).** Diphenyl hydrogen phosphate (41 mg, 0.164 mmol) was added to a solution of [Zn₂(XDK)(acac)₂(CH₃OH)₂]·H₂O (**6**·H₂O) (81 mg, 0.081 mmol) in methanol (10 mL)/methylene chloride (10 mL). The reaction mixture was stirred at room temperature for 1 h. The solvent was then removed by a rotary evaporator, and the residue was crystallized from a CH₃OH/Et₂O mixed solvent. Block-shaped colorless crystals were collected, washed with ether, and dried in vacuo (72 mg, 64%). Anal. Calcd for C₅₈H₆₈N₂O₁₉Zn₂P₂ (**8**): C, 54.00; H, 5.31; N, 2.17. Found: C, 53.59; H, 4.84; N, 2.27. IR (Nujol): 3460 (br), 1731, 1682 (s),

Table 2. Crystallographic and Experimental Data for [ZnM(XDK)(DPP)₂(CH₃OH)₂(H₂O)]·CH₃OH (**7**·CH₃OH, M = Co; **8**·CH₃OH, M = Zn)

	7 ·CH ₃ OH	8 ·CH ₃ OH
formula	C ₅₉ H ₇₂ N ₂ O ₂₀ ZnCoP ₂	C ₅₉ H ₇₂ N ₂ O ₂₀ Zn ₂ P ₂
fw	1315.48	1321.93
crystal system	monoclinic	monoclinic
space group	<i>P</i> 2 ₁ / <i>n</i>	<i>P</i> 2 ₁ / <i>n</i>
<i>a</i> , Å	18.812(2)	18.845(6)
<i>b</i> , Å	16.156(2)	16.105(3)
<i>c</i> , Å	21.760(2)	21.776(3)
β, deg	112.836(9)	112.78(2)
<i>V</i> , Å ³	6095(1)	6091(2)
<i>Z</i>	4	4
<i>T</i> , °C	-82	-74
<i>D</i> _{calcd} , g cm ⁻³	1.434	1.442
abs coeff, cm ⁻¹	7.94	9.16
transm factor	0.94–1.00	0.83–1.00
2θ range, deg	3 < 2θ < 46	3 < 2θ < 45
no. of unique data	8815	8296
no. of obsd data (<i>I</i> > 3σ(<i>I</i>))	5843	5189
no. of variables	767	767
<i>R</i> ^a	0.055	0.055
<i>R</i> _w ^a	0.064	0.061

^a $R = \sum ||F_o| - |F_c|| / \sum |F_o|$; $R_w = [\sum w(|F_o| - |F_c|)^2 / \sum w|F_o|^2]^{1/2}$, where $w = 1/\sigma^2(F_o)$.

1598 (s), 1592 (s), 1230, 1202 (s), 1116 (s), 933 (s), 764 (s), 722, 690 cm⁻¹. ¹H NMR (in CD₃OD at room temperature): δ 1.18 (s, 6H, Me), 1.27 (s, 12H, Me), 1.92 (s, 6H, *m*-Me), 2.80 (d, 4H, CH, *J* = 14 Hz), 1.58 (d, 2H, CH, *J* = 13 Hz), 2.13 (d, 2H, CH, *J* = 13 Hz), 7.0–7.3 (m, 22H, Ar). ³¹P{¹H} NMR (CD₃OD): δ -10.3 (s) (24 °C); δ -9.2 (s), -12.9 (s) (-75 °C).

Crystal Data and Intensity Measurements for [ZnM(XDK)(acac)₂(CH₃OH)₂] (2**, M = Co; **3**, M = Mn; **4**, M = Fe; **5**, M = Ni) and [ZnM(XDK){(PhO)₂PO₂}]₂(CH₃OH)₂(H₂O)]·CH₃OH (**7**·CH₃OH, M = Co; **8**·CH₃OH, M = Zn).** X-ray quality crystals were obtained by recrystallizations of (**2**–**5**)·H₂O from a minimum amount of methanol at room temperature or slow evaporation of concentrated methanolic solution. Those of (**7**, **8**)·CH₃OH were obtained by vapor diffusion of Et₂O into a methanolic solution of **7** or **8**. Crystal data and experimental conditions are listed in Tables 1 and 2. All data were collected on an Enraf-Nonius CAD4 diffractometer by using graphite monochromated Mo Kα (λ = 0.710 69 Å) radiation. Three standard reflections were monitored every ~200 reflections and showed no systematic decrease in intensity. Reflection data were corrected for Lorentz–polarization and absorption effects.

Table 3. Assignments of Metals in 2–5 and 7·CH₃OH

compd	site A ^a	site B ^b	R	R _w	B _{eq} (A), ^d Å ²	B _{eq} (B), ^d Å ²
2	Zn	Co	0.049	0.051	2.94	2.64 ^c
	Co	Zn	0.068	0.077	1.72	4.09
3	Zn	Mn	0.046	0.051	3.11	3.33 ^c
	Mn	Zn	0.083	0.115	1.23	5.85
4	Zn	Fe	0.041	0.049	2.82	2.75 ^c
	Fe	Zn	0.069	0.093	1.11	3.26
5	Zn	Ni	0.050	0.058	2.77	2.29 ^c
	Ni	Zn	0.058	0.071	2.01	3.07
7·CH ₃ OH	Zn	Co	0.055	0.064	2.27	3.03 ^c
	Co	Zn	0.066	0.082	1.24	4.36

^a Trigonal bipyramidal (2–5) or tetrahedral (7·CH₃OH) site. ^b Octahedral site. ^c Original assignments. ^d Anisotropic thermal parameters given as the isotropic equivalent displacement parameter defined as $B_{eq} = (8\pi^2/3)\sum_i U_{ij}a_i^*a_j^*a_i^*a_j^*$.

Structure Solution and Refinement. [ZnM(XDK)(acac)₂(CH₃OH)₂] (2, M = Co; 3, M = Mn). The structures were solved by direct methods with SHELXS-86.¹⁶ The zinc and heterometal atoms were located in the initial *E* map, and subsequent Fourier syntheses gave the positions of other non-hydrogen atoms. The structures were refined with the full-matrix least-squares techniques minimizing $\sum w(|F_o| - |F_c|)^2$. The coordinates of all hydrogen atoms were determined by difference Fourier synthesis and were fixed with an appropriate B_{iso} in the refinement. Final refinements with anisotropic thermal parameters for non-hydrogen atoms converged to $R = 0.049$ and $R_w = 0.051$ for 2 (M = Co) and $R = 0.046$ and $R_w = 0.051$ for 3 (M = Mn).

[ZnM(XDK)(acac)₂(CH₃OH)₂] (4, M = Fe; 5, M = Ni). The structures were solved by direct methods with SIR92¹⁷ and refined by procedures similar to those described for 3 and 4. The coordinates of hydroxyl hydrogen atoms of the coordinated methanol were determined by difference Fourier syntheses, and the other hydrogen atoms were calculated at the ideal positions with a C–H distance of 0.95 Å. Final refinements with anisotropic thermal parameters for non-hydrogen atoms converged to $R = 0.041$ and $R_w = 0.049$ for 4 (M = Fe) and $R = 0.050$ and $R_w = 0.058$ for 5 (M = Ni). Hydrogen atoms were not refined with appropriate B_{iso} .

[ZnM(XDK){(PhO)₂PO₂}]₂(CH₃OH)₂(H₂O)·CH₃OH (7·CH₃OH, M = Co; 8·CH₃OH, M = Zn). The structures were solved and refined as described for 4 and 5. The coordinates of oxygen-bound hydrogen atoms of the coordinated methanol and water molecules were determined by difference Fourier synthesis, and the other carbon-bound hydrogen atoms (except for those of solvent molecule) were calculated at the ideal positions by taking the C–H distance as 0.95 Å. Hydrogen atoms were assigned an appropriate B_{iso} value but not refined. Final refinements with anisotropic thermal parameters for non-hydrogen atoms converged to $R = 0.055$ and $R_w = 0.064$ for 7 (M = Co) and $R = 0.055$ and $R_w = 0.061$ for 8 (M = Zn).

Atomic scattering factors and values of f' and f'' for Zn, Co, Mn, Fe, Ni, O, N, and C were taken from the literature.¹⁸ All calculations were carried out on a Digital VAX Station 3100 or 4200 with the TEXSAN Program System.¹⁹ The perspective views were drawn by using the program ORTEP.²⁰ In the refinement of 2–5 and 7·CH₃OH, the metal ion assignments were confirmed by switching the Zn and M atoms. In all cases, R and R_w values were higher by 0.8–6.4% than those for the original assignments, and the differences between B_{eq} values for the two metal atoms increased to 1.1–4.6 (Table 3). Final atomic positional and thermal parameters for all atoms of 2–5, 7·CH₃OH, and 8·CH₃OH are supplied as Supporting Information.

Results and Discussion

Synthesis and Characterization of Heterodimetallic Complexes of XDK, [ZnM(XDK)(acac)₂(CH₃OH)₂] (M = Co, Mn, Fe, Ni). Recently, we reported the synthesis and characterization of a mononuclear zinc complex of XDK, [Zn(XDK)(H₂O)] (1), which was readily transformed to the dizinc compound [Zn₂(XDK)(acac)₂(CH₃OH)₂] (6) by treatment with Zn(acac)₂·2H₂O.¹¹ This methodology was applied in the present study to the preparation of heterodimetallic complexes formulated as [ZnM(XDK)(acac)₂(CH₃OH)₂] (Scheme 1). Reaction of 1 with Co(II)(acac)₂·2H₂O (acac = 2,4-pentanedionate) in refluxing methanol afforded pink crystals of [ZnCo(XDK)(acac)₂(CH₃OH)₂]·H₂O (2·H₂O) in good yield. The product composition was determined by elemental analysis and IR spectroscopy, which indicated the presence of both XDK (1728–1586 cm⁻¹) and acac (1520 cm⁻¹). An electronic spectrum of the compound in CHCl₃ exhibited absorption at 568 nm ($\epsilon = 39$ M⁻¹ cm⁻¹) characteristic of octahedral Co(II). Similar treatment of 1 with 1 equiv of M(acac)₂·2H₂O gave a series of heterodimetallic complexes, [ZnM(XDK)(acac)₂(CH₃OH)₂]·H₂O (3·H₂O, M = Mn; 4, M = Fe; 5·H₂O, M = Ni). The IR spectra of 3–5 closely resembled that of 2. The electronic absorption spectra of 4 (M = Fe) and 5 (M = Ni) showed broad bands centered at 442 nm ($\epsilon = 1.2 \times 10^3$ M⁻¹ cm⁻¹) and 688 nm ($\epsilon = 7.1$ M⁻¹ cm⁻¹), respectively, whereas that of 3 (M = Mn) lacked any characteristic features in the 300–800 nm range. The Zn^{II}Fe^{II} complex 4 is air-sensitive even in the solid state and was handled under a nitrogen atmosphere. Following reaction of 1 with Cu(acac)₂, we were unable to isolate the analogous heterodimetallic [ZnCu(XDK)(acac)₂(CH₃OH)₂] compound.

The structures of 2–5 were determined by X-ray crystallographic analysis to be isomorphous with that of [Zn₂(XDK)(acac)₂(CH₃OH)₂] (6). ORTEP drawings of complexes 2–5 with the systematic atomic numbering schemes as well as a summary of bond lengths and angles are given in Figures 1 and 2 and the Supporting Information. A summary of key structural features of 2–6 is presented in Table 4. The unit cells contain four discrete molecules without any noteworthy intermolecular contacts. Each molecule comprises divalent zinc and heterometal ions with one XDK, two acac, and two coordinated methanol ligands. The zinc atom occupies a five-coordinate, trigonal bipyramidal site, and the heterometal ion resides in an octahedral environment. There is no disorder between the two metal sites (Table 3), as confirmed by the absence of residual electron density or large thermal motion of the coordinated atoms. The heterodimetallic center is bridged by the two carboxylate groups of the XDK ligand and also asymmetrically by the O(3) atom of the acac ligand (Table 4). The metal–metal separations vary slightly according to the size of the metal in the octahedral site, being correlated linearly ($r = 0.970$) with the high-spin octahedral metal ion radii,²¹ as indicated in Figure 3. The two carboxylate groups are almost coplanar, with dihedral angles ranging from 3 to 6°, and are almost perpendicular to the [ZnMO(3)] plane. The metal atoms are displaced from the planes of the carboxylate groups, a common feature in dinuclear XDK complexes.^{12b} The extent of the out-of-plane distortion is given by the values of d (the distance from the metal atom to the dicarboxylate plane) and ϕ (the dihedral angle between the [ZnM(OCCO₂)₂] and the carboxylate planes), values for which are reported in Table 4. The Zn and M ions are located 0.43–0.46 and 1.19–1.21 Å,

(16) Sheldrick, G. M. *Crystallography Computing*; Oxford University Press: Oxford, U.K., 1985; p 175.

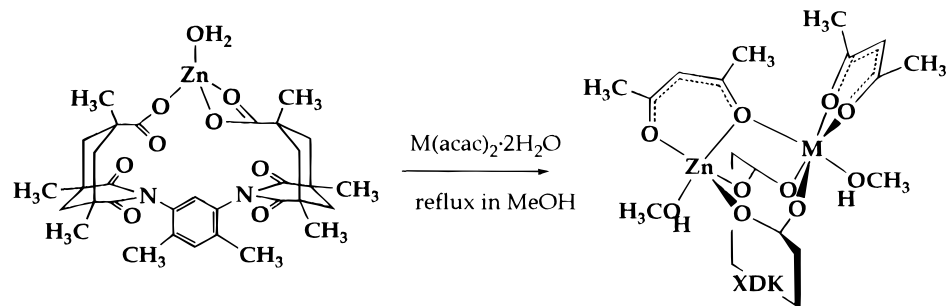
(17) Burla, M. C.; Camalii, M.; Cascarano, C.; Giacovazzo, C.; Polidori, G.; Spagna, R.; Viterbo, D. *J. Appl. Crystallogr.* **1989**, *22*, 389.

(18) (a) Cromer, D. T.; Waber, J. T. In *International Tables for X-ray Crystallography*; Kynoch Press: Birmingham, England, 1974; Vol. IV. (b) Cromer, D. T. *Acta Crystallogr.* **1965**, *18*, 17.

(19) *TEXSAN Structure Analysis Package*; Molecular Structure Corp.: The Woodlands, TX, 1985.

(20) Johnson, C. K. *ORTEP-II*; Oak Ridge National Laboratory: Oak Ridge, TN, 1976.

(21) Shannon, R. D.; Prewitt, C. T. *Acta Crystallogr.* **1969**, *B25*, 925.

Scheme 1^a

(1)

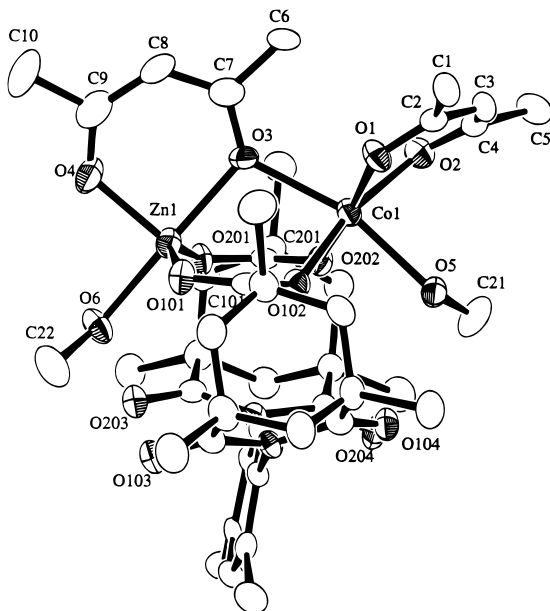
M = Co (2), Mn (3), Fe (4), Ni (5), Zn (6)^a^a Reference 11.

Figure 1. ORTEP diagram of $[\text{ZnCo}(\text{XDK})(\text{acac})_2(\text{CH}_3\text{OH})_2]$ (2). Thermal ellipsoids are drawn at the 40% probability level, and hydrogen atoms are omitted for clarity.

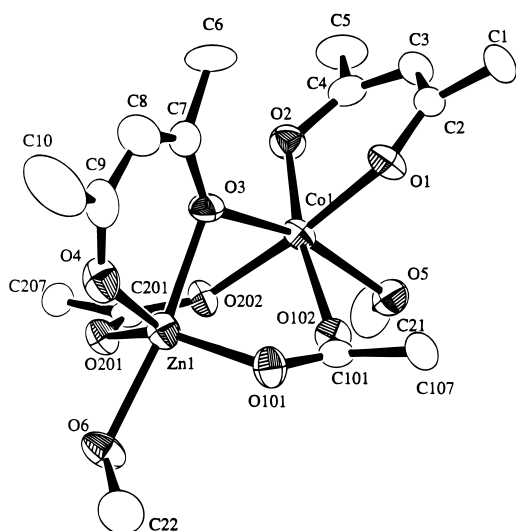


Figure 2. ORTEP plot of the dinuclear core of complex 2. Hydrogen atoms and all atoms of the XDK ligand, except for carboxylate groups, are omitted for clarity.

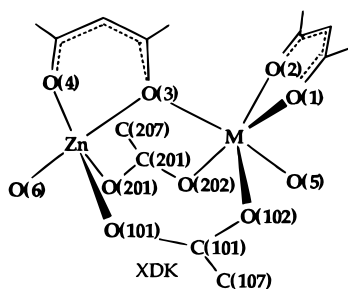
respectively, from the dicarboxylate plane, indicating that the distortion is more extensive for the heterometal than for zinc.

The stereochemistry of the trigonal bipyramidal zinc atom remains almost invariant irrespective of the heterometal atoms

in 2–5. Two carboxylate oxygen atoms of XDK ($\text{Zn}-\text{O}_{\text{CO}_2} = 1.953(4)-1.990(5)$ Å, average 1.971 Å), $\text{O}_{\text{CO}_2}-\text{Zn}-\text{O}'_{\text{CO}_2} = 142.0(2)-143.7(2)^\circ$, average 142.8°), and the terminal oxygen atom of the acac ligand ($\text{Zn}-\text{O}(4) = 1.955(5)-1.977(4)$ Å, average 1.965 Å) lie in the equatorial plane. The axial ligands are the bridging oxygen atom of the acac ligand ($\text{Zn}-\text{O}(3) = 2.129(4)-2.151(4)$, average 2.137 Å; $\text{O}(3)-\text{Zn}-\text{O}(4) = 90.3(2)-90.8(2)^\circ$, average 90.6°) and the oxygen atom of methanol ($\text{Zn}(1)-\text{O}(6) = 2.104(4)-2.110(4)$ Å, average 2.107 Å). The $\text{O}(3)-\text{Zn}(1)-\text{O}(6)$ angle is $168.6(2)-169.4(2)^\circ$, average 169.0° . The $\text{O}_{\text{CO}_2}-\text{Zn}-\text{O}'_{\text{CO}_2}$ bite angle is considerably expanded from an ideal value of 120° , yet there is almost no strain around the $\text{Zn}-\text{O}_{\text{CO}_2}-\text{C}_{\text{CO}_2}$ angle (average 121.0°). The six-membered chelate ring comprising of the acac ligand, $[\text{Zn}(1)\text{O}(3)\text{C}(7)\text{C}(8)\text{C}(9)\text{O}(4)]$, is planar and is nearly parallel to the $[\text{ZnMO}(3)]$ plane. The heterometal atom adopts a distorted octahedral geometry. The ligands are two carboxylate oxygen atoms of XDK ($\text{M}-\text{O}_{\text{CO}_2} = 2.037(4)-2.123(4)$ Å, average 2.075 Å; $\text{O}_{\text{CO}_2}-\text{M}-\text{O}'_{\text{CO}_2} = 92.5(2)-94.5(2)^\circ$, average 93.6°), two oxygen atoms of the chelating acac ($\text{M}-\text{O}(1), \text{O}(2) = 1.994(4)-2.115(4)$ Å, average 2.041 Å; $\text{O}(1)-\text{M}-\text{O}(2) = 85.0(2)-91.0(2)^\circ$, average 87.9°), and, in the axial sites, the bridging oxygen atom of acac and the oxygen atom of methanol ($\text{M}-\text{O}(3) = 2.142(4)-2.332(4)$ Å, average 2.238 Å; $\text{M}-\text{O}(5) = 2.122(4)-2.269(4)$ Å, average 2.195 Å; $\text{O}(3)-\text{M}-\text{O}(5) = 157.0(1)-164.7(1)^\circ$, average 161.3°). The geometrical distortion around the octahedral metal ion increases with the ionic radius of the heterometal, as revealed by the $\text{O}(3)-\text{M}-\text{O}(5)$ and $\text{O}(1)-\text{M}-\text{O}(2)$ angles. The six-membered acac chelate ring adopts an envelope conformation and is nearly perpendicular ($\sim 98^\circ$) to the $[\text{ZnMO}(3)]$ plane. The XDK ligand is somewhat distorted from idealized C_{2v} symmetry owing in part to weak hydrogen-bonding interactions ($2.810(5)-2.904(6)$ Å) between one of its imino oxygen atoms and the $\text{O}(5)$ and $\text{O}(6)$ atoms of coordinating methanol molecules.

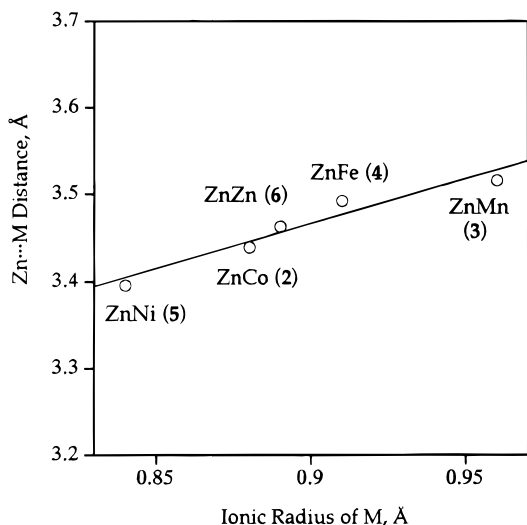
The present series of heterodimetallic complexes may be useful scaffolds for preparing synthetic models of metalloproteins having heterodinuclear metal sites. Calcineurin and kidney bean purple acid phosphatase (KBPAP) both house a dinuclear $\text{Zn}^{\text{II}}\text{Fe}^{\text{III}}$ center,^{5,6} and the purple acid phosphatase from porcine uteri (uteroferrin) can also function with a $\text{Zn}^{\text{II}}\text{Fe}^{\text{III}}$ set.²² Although the $\text{ZnFe}(\text{XDK})$ complex (4) has an oxidation state different from that in calcineurin and KBPAP, its sensitivity to dioxygen suggests that it might be possible to oxidize it to the requisite $\text{Zn}^{\text{II}}\text{Fe}^{\text{III}}$ level. The $\text{Zn}\cdots\text{Fe}$ separation of $3.492(1)$ Å in 4 is comparable to that of the phenoxo-bridged $\text{Fe}^{\text{III}}\text{Zn}^{\text{II}}$ complex $[\text{Fe}^{\text{III}}\text{Zn}^{\text{II}}(\text{BPMP})(\text{OAc})_2]^{2+}$ ($3.437(1)$ Å)^{9a,b} (HBPMP

(22) (a) David, S. S.; Que, L., Jr. *J. Am. Chem. Soc.* **1990**, *112*, 6455. (b) True, A. E.; Scarrow, R. C.; Randall, C. R.; Holz, R. C.; Que, L., Jr. *J. Am. Chem. Soc.* **1993**, *115*, 4246.

Table 4. Structural Parameters of $[\text{ZnM}(\text{XDK})(\text{acac})_2(\text{MeOH})_2]$ ($\text{M} = \text{Co}, \text{Mn}, \text{Zn}, \text{Fe}, \text{Ni}$)

	3 (M = Mn)	4 (M = Fe)	2 (M = Co)	6 (M = Zn) ^a	5 (M = Ni)
Zn...M, Å	3.517(1)	3.492(1)	3.440(2)	3.463(1)	3.397(1)
Zn-O(XDK) _{av} , Å ^b	1.986(6)	1.971(6)	1.966(6)	1.963(5)	1.963(6)
Zn-O(acac) _{ax} , Å	2.129(4)	2.132(4)	2.135(4)	2.131(3)	2.151(4)
Zn-O(acac) _{eq} , Å	1.977(4)	1.955(5)	1.964(5)	1.969(4)	1.962(5)
Zn-O(MeOH), Å	2.105(4)	2.110(4)	2.107(4)	2.117(4)	2.104(4)
M-O(XDK) _{av} , Å ^b	2.116(6)	2.082(6)	2.055(6)	2.056(4)	2.048(6)
M-O(acac) _{ax} , Å	2.332(4)	2.255(4)	2.224(5)	2.248(3)	2.142(4)
M-O(acac) _{eq} , Å ^b	2.113(6)	2.035(6)	2.021(6)	2.028(4)	1.997(6)
M-O(MeOH), Å	2.269(4)	2.198(4)	2.190(4)	2.195(4)	2.122(4)
Zn-O(3)-M, deg	104.2(2)	105.5(2)	104.2(2)	104.5(1)	104.6(2)
O(101)-Zn-O(201), deg	143.1(2)	142.2(2)	142.0(2)	141.8(1)	143.7(2)
O(3)-Zn-O(4), deg	90.3(2)	90.8(2)	90.6(2)	90.4(2)	90.8(2)
O(3)-Zn-O(6), deg	169.4(2)	169.2(2)	168.7(2)	168.3(1)	168.6(2)
O(102)-M-O(202), deg	93.3(2)	92.5(2)	94.5(2)	94.4(1)	94.0(2)
O(1)-M-O(2), deg	85.0(2)	87.0(2)	88.6(2)	89.4(1)	91.0(2)
O(3)-M-O(5), deg	157.0(1)	160.3(2)	163.2(2)	161.3(1)	164.7(1)
ϕ , deg ^c	27	27	27	27	28
$d(\text{Zn})$, Å ^d	0.45	0.46	0.46	0.46	0.43
$d(\text{M})$, Å ^d	1.20	1.21	1.19	1.18	1.21
[ZnMO(101)O(102)] vs [ZnMO(201)O(202)], deg ^e	48	49	49	49	51
[O(101)O(102)C(101)C(107)] vs [O(201)O(202)C(201)C(207)], deg ^e	3	5	5	5	6

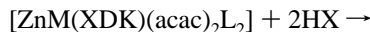
^a Reference 11. ^b Average value. Estimated deviations in parentheses are derived from $(\sigma_A^2 + \sigma_B^2)^{1/2}$. ^c Dihedral angle between the $[\text{ZnM}(\text{Oco}_2)_2]$ and the dicarboxylate planes (average value). ^d Distance from the metal atom to the dicarboxylate plane. ^e Dihedral angle.

**Figure 3.** Plots of Zn...M distance (Å) observed in 2–6 vs ionic radius of the high-spin octahedral M^{II} ion (Å).

= 2,6-bis[(bis(2-pyridylmethyl)amino)methyl]-4-methylphenol) but shorter than that in $[\text{Fe}^{\text{III}}\text{Zn}^{\text{II}}(\text{BPMP})\{(\text{PhO})_2\text{PO}_2\}_2]^{2+}$ (3.695(1) Å).²³ These values may be compared with the corresponding distances in calcineurin (3.0 Å)⁶ and KBPAP (3.1 Å).⁵ The structure of bovine lens leucine aminopeptidase (bLAP) has been determined by X-ray crystallography to contain

two carboxylate-bridged zinc ions with a Zn...Zn separation of 2.9 Å.⁴ One of the zinc ions can be replaced by other divalent cations such as Mg^{2+} , Mn^{2+} , and Co^{2+} , demonstrating that bLAP can function with $\text{Zn}^{\text{II}}\text{M}^{\text{II}}$ heterodimetallic cofactors ($\text{M} = \text{Mg}^{2+}$, Mn^{2+} , Co^{2+}). It was therefore of interest to examine the reactivities of the present ZnM heterodimetallic complexes with phosphate esters.

Reaction of $[\text{ZnM}(\text{XDK})(\text{acac})_2(\text{CH}_3\text{OH})_2]\cdot\text{H}_2\text{O}$ ($\text{M} = \text{Co}^{2+}$, Zn^{2+}) with Diphenyl Hydrogen Phosphate. In order to prepare phosphate ester derivatives, we exploited the leaving-group ability of the acac ligands in the ZnM(XDK) complexes under acidic conditions. As indicated in eq 1, substitution of



coordinated acac ($\text{p}K_a \sim 5$) occurs readily in the presence of stronger protic acids (HX) such as phosphoric acid esters ($\text{p}K_a \sim 2$). Accordingly, compounds 2 and 6 were allowed to react with diphenyl hydrogen phosphate ($(\text{PhO})_2\text{PO}_2\text{H} = \text{HDPP}$). Treatment of $[\text{ZnCo}(\text{XDK})(\text{acac})_2(\text{CH}_3\text{OH})_2]\cdot\text{H}_2\text{O}$ (2·H₂O) with 2 equiv of HDPP in a methanol/methylene chloride mixed solvent at room temperature afforded $[\text{ZnCo}(\text{XDK})\{(\text{PhO})_2\text{PO}_2\}_2(\text{CH}_3\text{OH})_2(\text{H}_2\text{O})]$ (7) in good yield (Scheme 2). Reaction of 2·H₂O with 1 equiv of HDPP similarly resulted in the formation of 7, albeit in lower yield. The products were characterized by elemental analysis, by IR spectroscopy, which indicated the presence of XDK (1731–1592 cm^{-1}), DPP (1228, 1201 cm^{-1}), and hydroxyl groups ($\sim 3479 \text{ cm}^{-1}$), and by UV-vis spectroscopy. The last revealed an absorption corresponding

(23) Schepers, K.; Bremer, B.; Krebs, B.; Henkel, G.; Althaus, E.; Mosel, B.; Müller-Warmuth, W. *Angew. Chem., Int. Ed. Engl.* **1990**, *29*, 531.

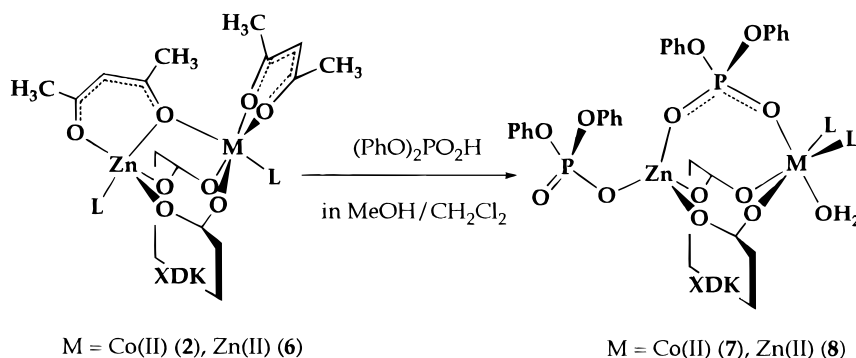
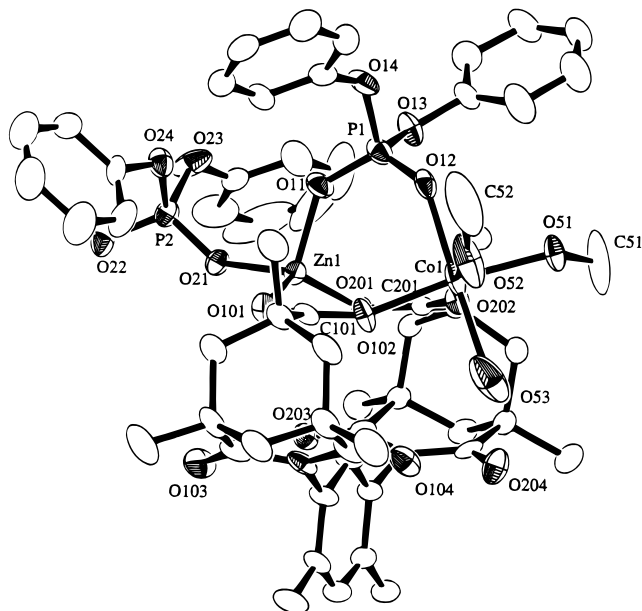
Scheme 2^a^a L = CH₃OH.

Figure 4. ORTEP view of [ZnCo(XDK)(DPP)₂(CH₃OH)₂(H₂O)] (7). Thermal ellipsoids are drawn at the 40% probability level, and hydrogen atoms are omitted for clarity.

to the d–d transition of Co(II) ions around 538 nm ($\epsilon = 17 \text{ M}^{-1} \text{ cm}^{-1}$), which is shifted by $\sim 980 \text{ cm}^{-1}$ to higher energy and is considerably weaker than the band in $2 \cdot \text{H}_2\text{O}$ (568 nm, $\epsilon = 39 \text{ M}^{-1} \text{ cm}^{-1}$).

The structure of $7 \cdot \text{CH}_3\text{OH}$, as determined by X-ray crystallography, is displayed as ORTEP drawings in Figures 4 and 5. Selected bond lengths and angles are given in Table 5. Compound **7** consists of divalent zinc and cobalt ions with one XDK, two DPP, two coordinated methanols, and one water. The ZnCo center is bridged by XDK through its two carboxylate groups and also by a diphenyl phosphate ligand. The five-membered ring formed by the bridging phosphate ester and the metal atoms has an envelope conformation with P(1) at the apex (Figure 5b). The intra-ring O(11)–P(1)–O(12) angle has expanded by $\sim 10^\circ$ from the ideal tetrahedral value to $118.7(3)^\circ$. Similar structural features have previously been observed in diiron complexes with bridging phosphate esters.^{24–26} The other DPP ligand is terminally coordinated to zinc in a monodentate fashion. A dinuclear complex with a terminally coordinated

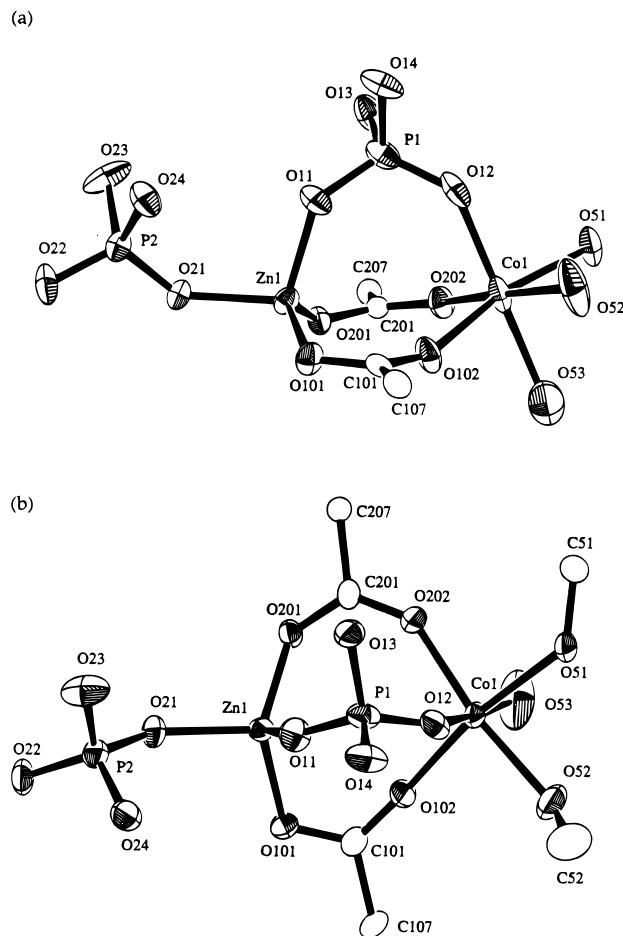


Figure 5. ORTEP plots of the dinuclear core of **7**, viewed (a) along and (b) perpendicular to the dicarboxylate plane. Thermal ellipsoids are drawn at the 40% probability level, and hydrogen atoms, phenyl groups of diphenyl phosphates, and all atoms of XDK, except for carboxylate groups, are omitted for clarity.

phosphate ligand is rare (Table 6), structurally characterized examples being [Fe₂Cl₂(η^1 -DPP)(TBPO)(MeOH)]²⁺ (HTBPO = *N,N,N',N'*-tetrakis(2-benzimidazolylmethyl)-2-hydroxy-1,3-diaminopropane)²⁷ and [Cu₂(β -ala)₄(η^1 -DPP)₂](DPP)₂ (β -ala = $-\text{OOC}(\text{CH}_2)_2\text{NH}_3^+$).²⁸ Some additional dinuclear transition metal complexes of phosphate esters are listed in Table 6.^{24–33} The Zn \cdots Co interatomic distance is 3.846(1) Å, which is longer by

(24) (a) Armstrong, W. H.; Lippard, S. J. *J. Am. Chem. Soc.* **1985**, *107*, 3730. (b) Turowski, P. N.; Armstrong, W. H.; Roth, M. E.; Lippard, S. J. *J. Am. Chem. Soc.* **1990**, *112*, 681.

(25) Turowski, P. N.; Armstrong, W. H.; Liu, S.; Brown, S. N.; Lippard, S. J. *Inorg. Chem.* **1994**, *33*, 636.

(26) Drücke, S.; Wiegardt, K.; Nuber, B.; Weiss, J.; Fleischhauer, H.-P.; Gehring, S.; Haase, W. *J. Am. Chem. Soc.* **1989**, *111*, 8622.

(27) Bremer, B.; Schepers, K.; Fleischhauer, P.; Haase, W.; Henkel, G.; Krebs, B. *J. Chem. Soc., Chem. Commun.* **1991**, 510.

(28) Glowiak, T.; Podgórska, I.; Baranowski, J. *Inorg. Chim. Acta* **1986**, *115*, 1.

(29) Krebs, B.; Schepers, K.; Bremer, B.; Henkel, G.; Althaus, E.; Müller-Warmuth, W.; Griesar, K.; Haase, W. *Inorg. Chem.* **1994**, *33*, 1907.

Table 5. Selected Bond Lengths (Å) and Angles (deg) of **7**·CH₃OH^a

Bond Lengths			
Zn(1)···Co(1)	3.846(1)		
Zn(1)–O(11)	1.930(4)	Zn(1)–O(21)	1.936(4)
Zn(1)–O(101)	1.947(4)	Zn(1)–O(201)	1.926(4)
Co(1)–O(12)	2.095(5)	Co(1)–O(51)	2.130(4)
Co(1)–O(52)	2.098(5)	Co(1)–O(53)	2.195(7)
Co(1)–O(102)	2.086(4)	Co(1)–O(202)	2.070(4)
P(1)–O(11)	1.479(4)	P(1)–O(12)	1.456(5)
P(1)–O(13)	1.595(5)	P(1)–O(14)	1.597(5)
P(2)–O(21)	1.485(4)	P(2)–O(22)	1.476(5)
P(2)–O(23)	1.583(5)	P(2)–O(24)	1.599(5)

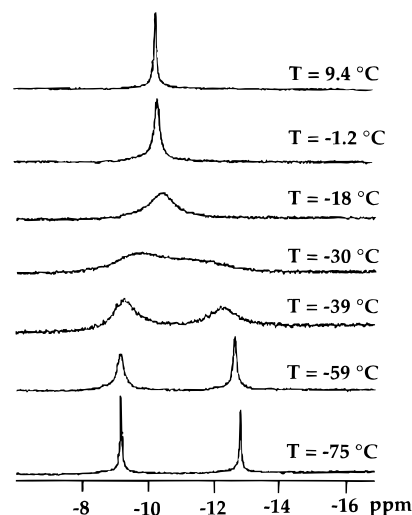
Bond Angles			
O(11)–Zn(1)–O(21)	102.8(2)	O(11)–Zn(1)–O(101)	106.2(2)
O(11)–Zn(1)–O(201)	106.3(2)	O(21)–Zn(1)–O(101)	103.6(2)
O(21)–Zn(1)–O(201)	108.9(2)	O(101)–Zn(1)–O(201)	126.6(2)
O(12)–Co(1)–O(51)	91.8(2)	O(12)–Co(1)–O(52)	90.7(2)
O(12)–Co(1)–O(53)	177.6(2)	O(12)–Co(1)–O(102)	96.2(2)
O(12)–Co(1)–O(202)	93.5(2)	O(51)–Co(1)–O(52)	83.6(2)
O(51)–Co(1)–O(53)	86.9(2)	O(51)–Co(1)–O(102)	168.3(2)
O(51)–Co(1)–O(202)	88.8(2)	O(52)–Co(1)–O(53)	91.1(3)
O(52)–Co(1)–O(102)	87.8(2)	O(52)–Co(1)–O(202)	171.4(2)
O(53)–Co(1)–O(102)	85.4(2)	O(53)–Co(1)–O(202)	84.5(2)
O(102)–Co(1)–O(202)	99.2(2)	O(11)–P(1)–O(12)	118.7(3)
O(11)–P(1)–O(13)	104.4(3)	O(11)–P(1)–O(14)	110.9(3)
O(12)–P(1)–O(13)	113.0(3)	O(12)–P(1)–O(14)	109.0(3)
O(13)–P(1)–O(14)	99.1(3)	O(21)–P(2)–O(22)	115.3(3)
O(21)–P(2)–O(23)	110.3(3)	O(21)–P(2)–O(24)	111.6(2)
O(22)–P(2)–O(23)	111.8(3)	O(22)–P(2)–O(24)	110.6(3)
O(23)–P(2)–O(24)	95.4(3)	Zn(1)–O(11)–P(1)	136.6(3)
Zn(1)–O(21)–P(2)	139.9(3)	Co(1)–O(12)–P(1)	136.2(3)
Zn(1)–O(101)–C(101)	116.0(4)	Zn(1)–O(201)–C(201)	134.7(4)
Co(1)–O(102)–C(101)	157.6(5)	Co(1)–O(202)–C(201)	143.9(4)

^a Estimated standard deviations are given in parentheses. See Figure 4 for atom labels.

0.406 Å than that found in the acac-bridged ZnCo complex **2** and by 0.151 Å than that of [Zn^{II}Fe^{III}(BPMP)(μ-η²-DPP)₂](ClO₄)₂ (3.695(1) Å). The two carboxylate groups of XDK are roughly coplanar with a dihedral angle of 10° and almost perpendicular to the [Zn(1)Co(1)P(1)O(11)O(12)] plane, the dihedral angle being 96°. The XDK ligand is slightly twisted, as observed in **2**–**5**. The Zn and Co atoms are located 0.74 and 0.58 Å, respectively, out of the plane defined by the two carboxylate groups.

The zinc atom is in a tetrahedral environment surrounded by the two carboxylate oxygen atoms of XDK, the oxygen atom of the bridging DPP, and that of the monodentate DPP. The cobalt atom adopts a less distorted octahedral geometry than that observed in **2**, being ligated by the two carboxylate oxygen atoms of XDK, the oxygen atom of the bridging DPP, and two methanol and one water molecules. The coordinated water molecule interacts weakly with the carbonyl oxygen atom of the imide moiety (O(53)···O(104) = 2.775(7) Å). In the crystal packing, a hydrogen-bonding network forms among the non-coordinated oxygen atom of the monodentate DPP ligand (O(22)), the oxygen atoms of the coordinated methanols (O(51), O(52)), and that of the solvent molecule (O(61)): O(22)···O(51) (*x* + 0.5, *−y* + 0.5, *z* + 0.5) = 2.663(6) Å, O(22)···O(61) (*x*, *y*, *z* + 1.0) = 2.727(8) Å, O(52)···O(61) (*x* − 0.5, *−y* + 0.5, *z* + 0.5) = 2.75(1) Å.

- (30) Norman, R. E.; Yan, S.; Que, L., Jr.; Backes, G.; Ling, J.; Sanders-Loehr, J.; Zhang, J. H.; O'Connor, C. J. *J. Am. Chem. Soc.* **1990**, *112*, 1554.
- (31) Jang, H. G.; Hendrich, M. P.; Que, L., Jr. *Inorg. Chem.* **1993**, *32*, 911.
- (32) Mahroof-Tahir, M.; Karlin, K. D.; Chen, Q.; Zubieta, J. *Inorg. Chim. Acta* **1993**, *207*, 135.
- (33) Hikichi, S.; Tanaka, M.; Moro-oka, Y.; Kitajima, N. *J. Chem. Soc., Chem. Commun.* **1992**, 814.

**Figure 6.** Variable-temperature ³¹P{¹H} NMR spectra of **8** in CD₃OD.

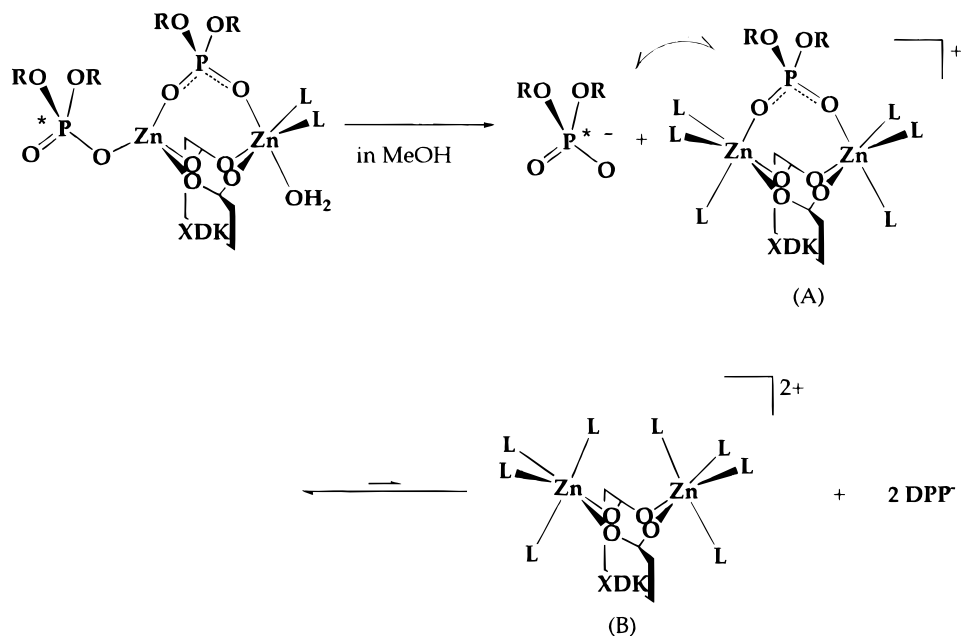
The analogous bis(phosphate)-substituted homodinuclear complex [Zn₂(XDK){μ-η²-(PhO)₂PO₂}{η¹-(PhO)₂PO₂}(CH₃OH)₂·(H₂O)] (**8**) was prepared by the reaction of [Zn₂-(XDK)(acac)₂(CH₃OH)₂·H₂O (**6**·H₂O)] with 2 equiv of diphenyl hydrogen phosphate in 64% yield. The structure was confirmed by X-ray crystallography to be isostructural with **7**. An ORTEP plot of the complex and some selected bond lengths and angles are provided in the Supporting Information: The structural features of the bridging and terminal phosphate ligands are quite similar to those observed in **7**. The Zn···Zn separation of 3.869(2) Å in **8** is almost identical to that of **7** and, notably, very close to the values found in the active sites of *E. coli* alkaline phosphatase complexed with inorganic phosphate (3.94 Å)² and of the Klenow fragment of DNA polymerase I complexed with nucleotides (3.9 Å).¹ Both enzymes can employ di- or trizinc ions to promote hydrolysis of phosphate ester bonds. Such hydrolysis reactions have been proposed to proceed through a two-metal-ion-promoted phosphoryl transfer mechanism. Since complex **8** appears to be a good synthetic model for these enzymes, the behavior of the phosphodiester ligands in solution was also examined (vide infra). Recently, structurally related dimagnesium complexes, [Mg₂(XDK){μ-η²-(PhO)₂PO₂}{η¹-(PhO)₂PO₂}(CH₃OH)₃(H₂O)] (**9**) and [Mg₂(XDK){μ-η²-DPP}(NO₃)(CH₃OH)₃(H₂O)] (**10**), were prepared and characterized in our laboratory.^{12c} Complex **9** has a bis-(phosphate) ligand geometry similar to those of **7** and **8**; however, one of the Mg atoms adopts trigonal bipyramidal rather than the tetrahedral geometry observed for Zn. The Zn···Zn separation in **8** is shorter than the Mg···Mg distances in **9** (4.108(3) Å) and **10** (4.240(5) Å).

The molar conductivity of **8** in methanol at 24 °C, 74 Ω^{−1}cm² mol^{−1}, corresponded to 1:1 electrolyte behavior, indicating that one diphenyl phosphate ligand is dissociated from the dimetallic center to generate a monocationic complex (**A**) and a free phosphate anion (Scheme 3). The ³¹P{¹H} NMR spectrum of **8** in CD₃OD at room temperature exhibited a singlet at δ = −10.3, and the ¹H NMR spectrum under the same conditions also showed the C_{2v} symmetrical spectral pattern of XDK ligand. These spectroscopic results suggested fluxional exchange between coordinated and free diphenyl phosphate anions. Variable-temperature ³¹P{¹H} NMR experiments were therefore carried out on **8** in CD₃OD. As illustrated in Figure 6, when the temperature is lowered, the singlet signal splits into two broad resonances. At the low-temperature limit, the ³¹P{¹H} NMR spectrum consists of two sharp singlets at δ = −9.2 and

Table 6. Dinuclear Metal Complexes Containing Phosphate Ester Ligands

complex	M...M, Å ^a	binding mode of P ^b	additional bridges ^c
[Fe ^{III} ₂ O(DPP) ₂ (HB(pz) ₃) ₂] ^d	3.335(1)	(μ-η ²) ₂	μ-oxo
[Fe ^{III} ₂ O(Ph ₂ PO ₂) ₂ (HB(pz) ₃) ₂] ^d	3.292(2)	(μ-η ²) ₂	μ-oxo
[Fe ^{III} ₂ O{(PhO)PO ₃ } ₂ (Me ₃ tacn) ₂] ^e	3.198(3)	(μ-η ²) ₂	μ-oxo
[Fe ^{III} ₂ O(TPA) ₂ (DPP)](ClO ₄) ₃ ^f	3.357(3)	(μ-η ²)	μ-oxo
[Fe ^{III} ₂ (BHPP)(DPP) ₂](BPh ₄) ^g	3.549(3)	(μ-η ²) ₂	μ-alkoxo
[Fe ^{III} ₂ (BHPMP)(DPP) ₂](ClO ₄) ^g	3.837(8)	(μ-η ²) ₂	μ-alkoxo
[Fe ^{III} ₂ (OH)(DPP) ₂ (HB(pz) ₃) ₂](BF ₄) ^h	3.586(1)	(μ-η ²) ₂	μ-hydroxo
[Fe ^{III} ₂ (OH)(Ph ₂ PO ₂) ₂ (HB(pz) ₃) ₂](BF ₄) ^h	3.5599(9)	(μ-η ²) ₂	μ-hydroxo
[Fe ^{III} ₂ (DPP) ₃ (HB(pz) ₃) ₂](BF ₄) ^h	4.6771(9)	(μ-η ²) ₃	none
[Fe ^{II} ₂ (BPMP)(DPP) ₂ Cl] ⁱ	3.683(4)	(μ-η ²) ₂	μ-alkoxo
[Zn ^{II} Fe ^{III} (BPMP)(DPP) ₂](ClO ₄) ₂ ^j	3.695(1)	(μ-η ²)	μ-alkoxo
[Cu ^{II} ₂ (UNO)(BNPP)](PF ₆) ₂ ^k	3.773(4)	(μ-η ²)	μ-alkoxo
[Zn ^{II} ₂ {(p-NO ₂ PhO)PO ₃ } ₂ {HB(<i>i</i> -Pr ₂ pz) ₃ } ₂] ^l	5.1	(μ-η ²)	none
7·CH ₃ OH ^m	3.846(1)	(μ-η ²)(η ¹)	(μ-carboxylato) ₂
8·CH ₃ OH ^m	3.869(2)	(μ-η ²)(η ¹)	(μ-carboxylato) ₂
[Mg ^{II} ₂ (XDK)(DPP)(NO ₃)(MeOH) ₃ (H ₂ O)] (10) ⁿ	4.240(5)	(μ-η ²)	(μ-carboxylato) ₂
[Mg ^{II} ₂ (XDK)(DPP) ₂ (MeOH) ₃ (H ₂ O)] (9) ⁿ	4.108(3)	(μ-η ²)(η ¹)	(μ-carboxylato) ₂
[Fe ^{III} ₂ Cl ₂ (TBPO)(DPP)(MeOH)](ClO ₄) ₂ ^o	3.700(2)	(η ¹)	μ-alkoxo
[Cu ^{II} ₂ (β-ala) ₄ (DPP) ₂](DPP) ₂ ^p	2.688(1)	(η ¹) ₂	(μ-carboxylato) ₄

^a Metal–metal separation (Å). ^b Mode of binding of phosphate esters to dinuclear metal center. ^c Additional bridging ligands other than phosphate esters. ^d Reference 24. HB(pz)₃ = hydrotris(1-pyrazolyl)borate. HDPP = diphenyl hydrogen phosphate. ^e Reference 26. Me₃tacn = 1,4,7-trimethyl-1,4,7-triazacyclononane. ^f Reference 30. TPA = tris(2-pyridylmethyl)amine. ^g Reference 29. H₃BHPP = 1,3-bis[(2-hydroxybenzyl)(2-pyridylmethyl)amino]-2-propanol. H₃BHPMP = 2,6-bis[[(2-hydroxybenzyl)(2-pyridylmethyl)amino)methyl]-4-methylphenol. ^h Reference 25. ⁱ Reference 31. HBPMP = 2,6-bis[bis(2-pyridylmethyl)amino)methyl]-4-methylphenol. ^j Reference 23. ^k Reference 32. HUNO = 2-[bis(2-pyridylethyl)amino]-methyl]-6-[bis(2-pyridylethyl)amino]phenol. HBNPP = bis(4-nitrophenyl) hydrogen phosphate. ^l Reference 33. HB(*i*-Pr₂pz)₃ = hydrotris(3,5-diisopropyl-1-pyrazolyl)borate. ^m This work. ⁿ Reference 12c. ^o Reference 27. HTBPO = *N,N,N',N'*-tetrakis(2-benzimidazolylmethyl)-2-hydroxy-1,3-diaminopropane. ^p Reference 28. β-ala = ⁻OOC(CH₂)₂NH₃⁺.

Scheme 3^a

^a L = CH₃OH or H₂O.

–12.9. The former peak was assigned to free DPP⁻, confirmed by addition of [Me₄N]DPP, and the latter, to coordinated DPP⁻. An upfield shift of the phosphate resonance occurs upon coordination to the dimetallic center.^{12c} Even at –51 °C, the ¹H NMR spectrum displayed the spectral pattern of XDK with C_{2v} symmetry, which strongly suggested a symmetrical (μ-DPP)-dizinc(II) structure for the monocationic species **A** (Scheme 3). The coalescence temperature is about –30 °C, from which can be estimated a free energy of activation of 45 kJ mol⁻¹ for the exchange reaction between bridging and free phosphate groups.³⁴ The intensity ratio of the two phosphorus resonances at –75

°C is not exactly 1:1, however. The intensity for the free DPP⁻ is slightly greater than that for the coordinated DPP⁻ (55:45), suggesting that some fraction of the bridging DPP⁻ ligand in **A** is further dissociated from the dinuclear center to generate a dicationic complex **B** (Scheme 3). A similar spectroscopic analysis of the structurally related dimagnesium complex **9** at the same concentration as that of **8** (30 mM) showed a coalescence temperature at 54 °C, corresponding to a free energy of activation of 60 kJ mol⁻¹.^{12c} These results suggested that the dizinc center in **8** is kinetically more labile than the dimagnesium center in **9** toward the diphenyl phosphate ligand, consistent with the known H₂O exchange rates of hydrated Zn²⁺ (~10⁷ s⁻¹) and Mg²⁺ (~10⁵ s⁻¹) ions.³⁵ This feature may be

(34) The values of ΔG[‡] (free activation energy) at coalescence temperature were calculated on the assumption of a 1:1 two-site-exchange model.

ascribed to the relatively smaller oxyphilicity or the lower charge density of the Zn(II) ion compared with Mg(II).

Conclusion

The mononuclear zinc complex [Zn(XDK)(H₂O)] (**1**) was demonstrated to be a useful precursor to a series of zinc-containing carboxylate-bridged heterodimetallic complexes. Dinuclear mixed-metal complexes, [Zn^{II}M^{II}(XDK)(acac)₂(CH₃OH)₂] (M: Co, **2**; Mn, **3**; Fe, **4**; Ni, **5**), were prepared by reaction of [Zn(XDK)(H₂O)] with M^{II}(acac)₂·2H₂O. The Zn···M distance is linearly correlated with the ionic radius of high-spin octahedral M^{II} ions. Carboxylate-bridged divalent heterodinuclear compounds are relatively rare and have potential utility as models for heterodimetallic centers in nonredox metalloenzymes. Complexes **2** and **6** (M = Co, Zn) were readily transformed to the novel bis(phosphate)-substituted

complexes [ZnM(XDK){μ-η²-(PhO)₂PO₂}{η¹-(PhO)₂PO₂}(CH₃OH)₂(H₂O)] (**7**, M = Co; **8**, M = Zn), having asymmetric (μ-phosphato)bis(μ-carboxylato)dimetal cores. The NMR spectroscopic and conductivity experiments on **8** demonstrated the lability of dizinc center toward phosphodiester ligands, leading to a ligand exchange process between bridging and free phosphate esters in methanol-*d*₄. These results provide useful information in connection with hydrolytic enzymatic reactions promoted by a two-metal-ion mechanism.

Acknowledgment. This work was supported by a grant from the National Science Foundation. T.T. is grateful to the Shigaku Shinko Zaidan for an International Research Fellowship.

Supporting Information Available: Tables of crystallographic and experimental data, complete atomic positional parameters, anisotropic temperature factors, and bond distances and angles for **2–5**, **7**·CH₃OH, and **8**·CH₃OH and ORTEP diagrams of **3–5** and **8** (88 pages). Ordering information is given on any current masthead page.

IC951625E

(35) Pan, T.; Long, D. M.; Uhlenbeck, O. C. In *The RNA World*; Gesteland, R. F., Atkins, J. F., Eds.; Cold Spring Harbor Laboratory Press: Plainview, NY, 1993; p 271.